ANL/CMT/CP-100737

ELECTROCHEMICAL CORROSION TESTING OF METAL WASTE FORMS*

by

D.P. Abraham, J.J. Peterson, and H.K. Katyal
Chemical Technology Division
Argonne National Laboratory-East
9700 South Cass Ave.
Argonne, IL 60439

and

D.D. Keiser and B.A. Hilton
Nuclear Technology Division
Argonne National Laboratory-West
Idaho Falls, ID 83403

RECEIVED
JAN 18 2000
OSTI

The submitted manuscript has been created by the University of Chicago as Operator of Argonne National Laboratory ("Argonne") under Contract No. W-31-109-ENG-38 with the U.S. Department of Energy. The U.S. Government retains for itself, and others acting on its behalf, a paid-up, nonexclusive, irrevocable worldwide license in said article to reproduce, prepare derivative works, distribute copies to the public, and perform publicly and display publicly, by or on behalf of the Government.

*To be published in the Proceedings of Corrosion 2000 (NACE Publications), Orlando, Florida, March 26-31, 2000

DISCLAIMER

This report was prepared as an account of work sponsored by an agency of the United States Government. Neither the United States Government nor any agency thereof, nor any of their employees, make any warranty, express or implied, or assumes any legal liability or responsibility for the accuracy, completeness, or usefulness of any information, apparatus, product, or process disclosed, or represents that its use would not infringe privately owned rights. Reference herein to any specific commercial product, process, or service by trade name, trademark, manufacturer, or otherwise does not necessarily constitute or imply its endorsement, recommendation, or favoring by the United States Government or any agency thereof. The views and opinions of authors expressed herein do not necessarily state or reflect those of the United States Government or any agency thereof.

DISCLAIMER

Portions of this document may be illegible in electronic image products. Images are produced from the best available original document.

ELECTROCHEMICAL CORROSION TESTING OF METAL WASTE FORMS

D. P. Abraham, J. J. Peterson and N. K. Katyal
Chemical Technology Division
Argonne National Laboratory
Argonne, IL 60439

D. D. Keiser and B. A. Hilton
Nuclear Technology Division
Argonne National Laboratory-West
Idaho Falls, ID 83403

ABSTRACT

Electrochemical corrosion tests have been conducted on simulated stainless steel-zirconium (SS-Zr) metal waste form (MWF) samples. The uniform aqueous corrosion behavior of the samples in various test solutions was measured by the polarization resistance technique. The data show that the MWF corrosion rates are very low in groundwaters representative of the proposed Yucca Mountain repository. Galvanic corrosion measurements were also conducted on MWF samples that were coupled to an alloy that has been proposed for the inner lining of the high-level nuclear waste container. The experiments show that the steady-state galvanic corrosion currents are small. Galvanic corrosion will, hence, not be an important mechanism of radionuclide release from the MWF alloys.

Keywords: stainless steel, zirconium, polarization resistance, galvanic corrosion, nuclear waste

INTRODUCTION

High-level nuclear waste forms are being produced at Argonne National Laboratory (ANL) for the disposal of waste resulting from the electrometallurgical treatment of the Experimental Breeder Reactor-II (EBR-II) spent fuel [1]. The transuranic elements and active fission products[1] that accumulate in the molten electrolyte salt are immobilized by blending the waste salt with zeolite and glass, and consolidated by hot pressing the mixture to form a

[1] Active fission products are oxidized to form salts in the electrorefiner and include alkali, alkaline earths, rare earths, and halogens.

monolithic ceramic waste form [2]. The stainless steel cladding, noble metal fission products (NMFP)[2] and actinide elements that are inert during the process are left behind in the anode baskets of the electrorefiner; these are consolidated by melting at 1600°C to form stainless steel-zirconium waste form alloys. The baseline metal waste form (MWF) is a SS-15Zr alloy; however, the zirconium content of the alloy is expected to range from 5 to 20 wt% [3]. The NMFP content of the MWF may range from 0.5 to 4 wt% and the actinide content from 2 to 10 wt% (mostly in the form of uranium). Both the ceramic and metal waste forms are intended for disposal in a geologic repository.

For acceptance in a repository, all nuclear waste forms must meet applicable performance requirements. An extensive testing program is underway at ANL to evaluate the corrosion behavior, mechanical and thermophysical properties, and phase stability of the ceramic and metal waste forms. The testing approach is based on the methodology outlined in the American Society for Testing of Materials document ASTM C 1174-91. The tests are intended to provide material property information, address repository-related requirements of the U.S. Department of Energy, and support development of radionuclide release models.

Corrosion resistance and, especially, the ability to retain radionuclides are primary indicators of waste form performance [4]. Radionuclide release from the MWF will depend on three interrelated factors: alloy metallurgy, degradation mechanisms, and environmental conditions in the repository. Since preliminary data showed that the corrosion behavior of MWF alloys is similar to that of stainless steels, an empirical model based on stainless steel data had been developed to provide a best estimate of MWF corrosion rates in a repository environment. The empirical parameters of the model will be adjusted, as new experimental data become available from the corrosion testing of MWF alloys.

This article presents room-temperature test data from two processes that may contribute to MWF degradation: uniform aqueous corrosion and galvanically enhanced corrosion. Uniform aqueous corrosion is expected to be one of the main mechanisms of radionuclide release from the MWF once the waste package container is breached. The behavior in various test solutions was studied by the polarization resistance method (based on ASTM G-59). The galvanic corrosion study was pursued to evaluate the corrosion behavior of MWF alloys galvanically coupled to alloy C-22[3] (UNS No. N06022), which is a candidate material for the inner lining of the proposed high-level nuclear waste container.

EXPERIMENTAL DETAILS

Test Equipment

The corrosion cell for the polarization resistance measurements included a round-bottomed flask, a flat specimen holder designed to accept specimens up to 16 mm in diameter and 3 mm thick, graphite auxiliary electrodes, and a saturated calomel electrode which served as the reference electrode. The applied potential and resulting current were measured by a Versastat-II potentiostat/galvanostat. The equipment was computer-controlled using SoftCorr III corrosion measurement software.[4]

A modified EG&G flat cell was used to determine the galvanic interaction between the metal specimens. Equal areas (1 cm^2) of the working electrode (test specimen) and counter electrode (C-22), separated by a distance of 12 cm, were exposed to the test solution. Galvanic contact between the electrodes was established by short-circuiting them through a computer-controlled potentiostat, which acted as a zero-resistance ammeter. A Ag/AgCl reference electrode (containing saturated KCl/AgCl solution) was used to measure the working electrode potential. Both galvanic current and potential were measured as a function of time for test periods up to 7 days; all potentials are expressed in the scale of the Ag/AgCl electrode.

---

[2] Noble metal fission products (NMFP) are inert during electrorefining and include Tc, Rh, Ru, Pd and Nb.

[3] C-22 is a trademark of Haynes International, Inc.

[4] Electrochemical instrumentation and software were purchased from EG&G Instruments, Princeton, NJ.

At the end of each test, the specimens were cleaned and examined for corrosion damage resulting from the galvanic interaction.

Test Samples

The MWF samples evaluated by the polarization resistance method contained 0 to 20 wt% Zr, up to 4 wt% simulated NMFP, up to 2 wt% Tc, and up to 11 wt% U. All samples were polished to a 600-grit finish and immersed in test solution for at least a half hour before the experiment. The external potential was applied at a rate of 0.6 V/h (0.16 mV/s), and the current was recorded continuously. Galvanic corrosion tests were conducted on nonradioactive samples that were polished to a 600-grit finish before exposure to the test solution.

Test Solutions

The baseline solution for our experiments was simulated J-13 solution, which represents the groundwater at the proposed Yucca Mountain repository [5].. Acid (pH=2 and pH=4) and base (pH=10) solutions were prepared by adding hydrochloric acid and sodium hydroxide, respectively, to the simulated J-13 composition. Typical compositions of the test solutions are shown in Table 1. Tests were conducted in solutions exposed to the laboratory atmosphere.

In an electrochemical cell, the solution resistance between the working and reference electrodes is known as the ohmic (or uncompensated) resistance, R_Ω. This resistance prevents the reference electrode from sensing the true potential at the specimen. Instead, it senses the applied voltage minus the iR drop due to solution resistance and transmits a distorted reading of the effective potential to the controlling potentiostat. Thus, an error is introduced into the measurement. This error is important only if R_Ω is a significant fraction of the polarization resistance, R_p [6].

The ohmic resistances in the test solutions were estimated by measuring solution conductivity [7] with a YSI Model 35 conductivity meter. Specific resistance of the solution was calculated as the reciprocal of the conductivity. Typical ohmic resistances, calculated assuming a specimen surface area of 1 cm^2 and a 1 mm distance between the working and reference electrode, are shown in Table 2. It is evident that for MWF alloys, the measured resistance, R, is roughly three orders of magnitude larger than R_Ω. For mild steel, R is one to two orders magnitude larger than R_Ω. Since $R = R_p + R_\Omega$, and since $R >> R_\Omega$, $R = R_p$ in our experiments. Hence, techniques to compensate for the ohmic drop were not used in our experiments.

Polarization measurements on nonradioactive samples were also conducted in 1000 ppm chloride, 10,000 ppm chloride, and concentrated J-13 solutions. These solutions represent stringent conditions that may be encountered by the waste forms during the repository lifetime. Typical solution compositions are shown in Table 3. The 1000 ppm and 10,000 ppm chloride solutions were prepared by adding sodium chloride to deionized water. The concentrated J-13 solution was used to examine the effect of high chloride and bicarbonate contents on MWF corrosion behavior.

RESULTS AND DISCUSSION

Polarization Resistance Measurements

In the polarization resistance method, the corrosion current is related to the slope of the potential-current plot through equation (1) [6]:

$$\frac{\Delta E}{\Delta I} = Rp = \frac{\beta_a \beta_c}{2.3(i_{corr})(\beta_a + \beta_c)} \qquad (1)$$

where

R_p = polarization resistance, Ω

β_a, β_c = anodic and cathodic Tafel constants (assumed to be 0.1V)

i_{corr} = corrosion current, A

The corrosion rates were calculated from the corrosion current from equation (2) [6]:

$$\text{Corrosion rate } (\mu m/y) = 25.4 \frac{0.13\, I_{corr}\, (\text{Eq.Wt.})}{d} \qquad (2)$$

where

μm/y = micrometers per year

I_{corr} = corrosion current density, $\mu A/cm^2$

Eq.Wt. = equivalent weight of corroding species, g

d = density of corroding species, g/cm^3

The equivalent weight and density values used in our calculations are listed in Table 4. The equivalent weights for the nonradioactive samples were calculated based on a procedure suggested in [6]; the densities listed are either measured values or have been obtained from literature. The equivalent weights and densities for all radioactive samples were assumed to be 24.9 g and 7.6 g/mL, respectively.

Average corrosion rates and standard deviations from triplicate tests on nonradioactive MWF specimens are shown in Table 5. It is evident that the corrosion rates for the MWF samples are comparable with the rates for 316 stainless steel and C-22. The corrosion rates of AISI 1018 (mild steel) samples are one to two orders of magnitude higher than rates for the MWF alloys. Corrosion rates are also affected by solution pH. The rates in simulated J-13 (pH~9) and pH=10 solutions are similar; rates are higher in acidic solutions. The corrosion rates in pH=2 solution are at least an order of magnitude greater than the rates in pH=10 solution.

Average corrosion rates and standard deviations from triplicate tests on MWF samples containing U and Tc are shown in Table 6. It is evident that the corrosion rates for U- and Tc-bearing MWF samples are similar to those measured for the nonradioactive samples; this is shown graphically in Fig. 1.

Average corrosion rates and standard deviations from triplicate tests in 1000 ppm chloride, 10,000 ppm chloride, and concentrated J-13 solutions are shown in Table 7. In general, the corrosion rates in these solutions are 5 to 10 times larger than rates measured in the simulated J-13 solution. The MWF corrosion rates are comparable to those measured for SS316 and C-22, and roughly two orders of magnitude lower than the rates for AISI 1018 in 1000 and 10,000 ppm chloride solutions. In concentrated J-13 solution, the mild steel samples display rates comparable to those for the MWF alloys. This finding suggests that mild steel is passivated by the high bicarbonate content of the solution.

Galvanic Corrosion Measurements

Tests in J-13 solution. Figure 2 shows a plot of galvanic potential versus time for specimens from AISI 1018, SS15ZR17 (SS-15Zr), and SS15ZR25 (SS-15Zr-1Nb-1Pd-1Rh-1Ru) alloys coupled to C-22 in J-13 (pH ~9) solution. The galvanic potential for AISI 1018 decreased with time and attained a steady-state value of ~-600 mV. In contrast, the galvanic potential for SS15ZR25 increased with time and reached a steady-state value of ~60 mV after 2 days. The galvanic potential of the SS15ZR17 specimen showed an initial increase, then decreased to a steady value of ~-200 mV.

A plot of galvanic current versus time for the AISI 1018 steel specimen is shown in Fig. 3. The current reached a maximum value of ~10 μA after 1 day, then decreased slowly to ~5 μA after 6 days. The oscillating nature of the current may be due to the formation and spallation of oxidation products formed on the steel surface. Optical examination showed that the C22 specimen was slightly discolored during the test. A spotty red corrosion layer was observed on the steel surface. X-ray diffraction of this layer suggested that the corrosion product is amorphous. However, the X-ray diffraction was performed *exsitu* (i.e., after the sample had been removed from the aqueous environment where the corrosion product had formed). *Insitu* analysis may be needed to identify the true nature of the corrosion product, because removal from the solution may have altered the layer in some manner, such as by the removal of the water of hydration.

A plot of galvanic current versus time for SS15ZR17 and SS15ZR25 specimens is shown in Fig. 4. An initial positive current (~0.06 μA) was observed for both specimens (in contrast to the negative current observed for AISI 1018), indicating that the waste form specimens were noble to Alloy C22. The current decreased rapidly and attained steady, near-zero values after a day. All specimens tested (i.e., C-22, SS15ZR17, and SS15ZR25) showed minor discolorations; microscopic pits were also observed on SS15ZR25.

Tests in pH=2 solution. The galvanic potentials measured at metallic specimens tested in pH=2 solution are shown in Fig. 5. The plots for the various specimens are very similar to those obtained in J-13 solution. The potential for the AISI 1018 specimen decreased with time and attained a steady-state value of ~-565 mV. The SS15ZR25 potential increased with time and reached a steady potential of ~295 mV. The potential of SS15ZR17 showed an initial increase, then decreased to a steady value of ~-45 mV. Note that the values of the steady-state potential measured in pH=2 solution are more positive than the values measured in J-13 solution. Table 8 compares the test results for the pH=2 and J-13 solutions.

The galvanic currents measured in pH=2 solution were also greater than those in J-13 solution. Figure 6 shows the galvanic current determined for the carbon steel specimen in pH=2 solution; the data for J-13 solution are shown for comparison. The current at pH=2 decreased from an initial value of about -150 μA to a steady-state value of ~-45 μA after about 4 days. The periodic oscillations of the current were similar (but much larger in magnitude) to those observed in the J-13 solution. Post-test examination showed that the carbon steel specimen was covered by a black layer. As was the case for the specimen tested in J-13, X-ray diffraction indicated that the corrosion product was amorphous.

The galvanic currents for SS15ZR17 and SS15ZR25 specimens in pH=2 solution are shown in Fig. 7. These alloys were electrochemically noble to C22. The initial values of the currents (0.85 μA for SS15ZR17 and 0.9 μA for SS15ZR25) were roughly an order of magnitude greater those observed in J-13 solution. The currents decreased and attained very small steady-state values (1 to 6 nA) in 1 to 2 days. However, Table 8 shows that these steady-state currents were 5 to 6 times greater than those measured for the alloys in J-13 solution. Post-test optical examination revealed no visible corrosion on any of the specimens.

CONCLUSIONS

Polarization resistance measurements on samples of SS-Zr metal waste forms have shown that their corrosion rates in groundwaters representative of the Yucca Mountain site (simulated J-13 solution) are very small. The rates are similar for samples containing 5-20 wt% Zr and up to 4 wt% simulated noble metal fission products. Alloy corrosion rates are not affected by the addition of up to 2 wt% Tc and up to 11 wt% U. The MWF corrosion rates are comparable in magnitude to those for 316 stainless steel and Alloy C22 in a variety of test solutions. For both nonradioactive and radioactive samples, the corrosion rates in pH=2 solution are roughly an order of magnitude greater than those in simulated J-13 solution.

Electrochemical galvanic corrosion tests were conducted on MWF alloys and a mild steel specimen. The samples were galvanically coupled to Alloy C22 in J-13 and pH=2 solutions. The SS-15Zr alloys were noble to C22, and the steady-

state corrosion currents measured were very small. The data indicate that enhanced corrosion due to galvanic coupling with the inner lining of the waste form container is not likely for the SS-15Zr waste form.

ACKNOWLEDGMENTS

This work was supported by the U.S. Department of Energy, Nuclear Research and Development Program, under Contract No. W-31-109-ENG-38.

REFERENCES

1. R.W. Benedict, Spent Fuel Treatment Demonstration Final Report, Argonne National Laboratory Report, NT-106 (1999).

2. C. Pereira, M. Hash, M. Lewis, and M. Richmann, JOM 49 (1997) p. 34.

3. S.M. McDeavitt, D.P. Abraham, and J.Y. Park, J. Nucl. Mater. 257 (1998) p. 21.

4. W. Lutze and R. C. Ewing, Radioactive Waste Forms for the Future, North-Holland, Amsterdam, (1988).

5. J.E. Harrar, J.F. Carley, W.F. Isherwood and E. Raber, UCID-21867, Lawrence Livermore National Laboratory (1990).

6. D.A. Jones, Principles and Prevention of Corrosion, Macmillan Publishing, New York, NY (1992).

7. Section 2510, Conductivity, Standard Methods for the Examination of Water and Waste Water, 18th Edition, M.H. Franson, ed., American Public Health Association, Washington, DC (1992) pp. 2-43.

TABLE 1
TYPICAL COMPOSITION OF SOLUTIONS USED FOR ELECTROCHEMICAL TESTING

pH	Solution Composition (mg/L)								
	Na	K	Ca	Mg	Si	SO_4^{-2}	Cl^{-1}	NO_3^{-1}	HCO_3^{-1}
2	49.1	5.1	10.9	2.12	35.1	17.8	443	10.5	4.4
4	48.9	5.16	10.8	2.11	33.5	18.2	88	10.2	5
9 (J-13)	50.9	5.21	10.2	2.09	33.8	18	4.31	10.1	109
10	65.2	5.32	10.4	2.18	37.9	18	4.33	9.5	88

TABLE 2
TYPICAL OHMIC AND POLARIZATION RESISTANCES ENCOUNTERED DURING ELECTROCHEMICAL TESTING

Solution pH	Solution Conductivity (mho/cm)	Specific Resistance (ohm-cm)	Ohmic Resistance (ohm)	Measured Resistance (ohm)	
				Typical MWF[a]	Mild Steel
2	4.23×10^{-3}	236.4	23.6	60.8×10^{3}	18.8×10^{1}
4	3.79×10^{-4}	2638	264	217.9×10^{3}	114×10^{2}
9 (J-13)	2.84×10^{-4}	3521	352	1121×10^{3}	123×10^{2}
10	3.05×10^{-4}	3279	328	977.1×10^{3}	379×10^{2}
Deionized water	-	18.8×10^{6}	-	-	-

[a]Calculated values are for SS-15Zr-1Nb-1Pd-1Rh-1Ru samples.

TABLE 3

HIGH CHLORIDE SOLUTIONS USED FOR CORROSION RATE MEASUREMENTS

Solution	pH	Solution Composition (mg/L)								
		Na	K	Ca	Mg	Si	SO_4^{-2}	Cl^{-1}	NO_3^{-1}	HCO_3^{-1}
1000 ppm Cl	5.8	607	-	-	-	-	-	1000	-	-
10,000 ppm Cl	6.3	6270	-	-	-	-	-	10000	-	-
Conc. J-13	8.2	5300	510	6	1.9	30	22	727	11	12700

TABLE 4

COMPOSITION, DENSITY AND EQUIVALENT WEIGHT OF TESTED SAMPLES

	Nominal Composition, wt%	Density, g/mL	Eq.Wt, g
SS316	SS316	8	25.5
SS15ZR17	SS-15Zr	7.65	24.9
SS05ZR18	SS-5Zr-2Nb-1Pd-1Ru	7.8	25.2
SS20ZR19	SS-20Zr-2Nb-1Pd-1Ru	7.7	24.8
SS15ZR26	SS-15Zr-1Nb-1Pd-1Rh-1Ru	7.8	24.9
C-22	Ni-21Cr-13Mo-4Fe-3W-2Co	8.7	26
AISI 1018	Fe-0.18C-0.8Mn-0.18Si	7.9	27.9

TABLE 7

CORROSION RATES MEASURED IN HIGH CHLORIDE SOLUTIONS

Sample	Nominal Composition	Room-Temperature Corrosion Rate (μm/y)					
		1000 ppm Cl^-		10,000 ppm Cl^-		Conc. J-13	
		Avg.[a]	SD[b]	Avg.	SD	Avg.	SD
Disc	SS316	1.70	0.65	2.31	1.41	2.18	1.40
SS15ZR17	SS-15Zr(as-cast)	0.91	0.18	0.94	0.51	0.70	0.25
SS05ZR18	SS-5Zr-2Nb-1Ru-1Pd	0.70	0.56	0.75	0.86	1.25	1.00
SS20ZR19	SS-20Zr-2Nb-1Ru-1Pd	0.99	0.59	2.12	1.62	1.80	0.91
SS15ZR26	SS-15Zr-1Nb-1Ru-1Pd-1Rh	0.52	0.17	1.53	1.89	2.18	2.02
C-22	Ni-21Cr-13Mo-4Fe-3W-2Co	0.56	0.04	0.81	0.56	0.88	0.38
AISI 1018	Fe-0.18C-0.8Mn-0.18Si	105	24	176	14	2.20	0.19

[a]Average of 3 measurements [b]Standard Deviation (1σ) of 3 measurements

TABLE 8

SUMMARY OF GALVANIC CORROSION TESTS ON METALLIC SPECIMENS COUPLED TO C-22

Ingot	Composition	Solution	Duration, d	E_{ss}, mV	I_{ss}, μA	Comments on Specimen
AISI 1018	Fe-0.18C-0.8Mn	J-13	6.09	-600	-5	Spotty red layer covering entire surface
		pH=2	6.97	-565	-45	Black layer covering entire surface
SS15ZR17	SS-15Zr	J-13	6.89	-200	0.002	Corrosion ring at boundary of Teflon ring
		pH=2	6.87	-45	0.01	No visible signs of corrosion
SS15ZR25	SS-15Zr-1Nb-1Pd-1Rh-1Ru	J-13	6.81	62	0.001	Small pits on surface
		pH=2	5.97	295	0.006	No visible signs of corrosion

E_{ss}: steady-state specimen potential. I_{ss}: steady-state galvanic current.

TABLE 5

CORROSION RATES MEASURED IN TEST SOLUTIONS WITH pH FROM 2 TO 10

Sample	Nominal Composition	Room-Temperature Corrosion Rate (μm/y) at pH value of							
		2		4		9 (J-13)		10	
		Avg.[a]	SD[b]	Avg.	SD	Avg.	SD	Avg.	SD
Disc	SS316	3.43	3.10	1.93	1.65	0.42	0.15	0.34	0.12
SS15ZR17	SS-15Zr	4.24	2.22	1.85	0.77	0.12	0.05	0.17	0.06
SS05ZR18	SS-5Zr-2Nb-1Ru-1Pd	8.51	2.23	2.78	2.18	0.12	0.05	0.25	0.11
SS20ZR19	SS-20Zr-2Nb-1Ru-1Pd	2.51	0.96	1.23	1.26	0.19	0.02	0.23	0.07
SS15ZR26	SS-15Zr-1Nb-1Ru-1Pd-1Rh	3.00	0.78	1.57	0.87	0.19	0.07	0.16	0.01
C-22	Ni-21Cr-13Mo-4Fe-3W-2Co	1.04	0.55	0.71	0.26	0.17	0.08	0.27	0.17
AISI 1018	Fe-0.18C-0.8Mn-0.18Si	1332	132	29.8	1.72	16.9	6.64	10.5	9.03

[a]Average of 3 measurements. [b]Standard Deviation (1σ) of 3 measurements.

TABLE 6

CORROSION RATES OF MWF SAMPLES CONTAINING U AND Tc

Sample	Nominal Composition	Room-Temperature Corrosion Rate (μm/y) at a pH value of							
		2		4		9 (J-13)		10	
		Avg.[a]	SD[b]	Avg.	St. Dev.	Avg.	St. Dev.	Avg.	St. Dev.
60	SS-15Zr-5U-2Tc	5.42	1.69	0.43	0.22	0.24	0.12	0.37	0.05
41	SS-15Zr-1Nb-1Rh-1Ru-1Pd-2U-1Tc	2.82	0.83	0.39	0.12	0.32	0.10	0.32	0.12
47	SS-15Zr-1Nb-1Rh-1Ru-1Pd-1Tc	0.75	0.08	0.41	0.16	0.38	0.16	0.55	0.14
53-55	SS-20Zr-1Nb-1Rh-1Ru-1Pd-1Tc	2.09	1.53	0.34	0.12	0.23	0.09	0.40	0.10
58	SS-5Zr-1Nb-1Rh-1Ru-1Pd-1Tc	8.53	4.10	0.37	0.13	0.37	0.14	0.32	0.10
64	SS-15Zr-0.6Ru-0.1Pd-11U-0.3Tc	9.06	1.50	0.66	0.21	0.39	0.06	0.71	0.23

[a]Average of 3 measurements [b]Standard Deviation (1σ) of 3 measurements

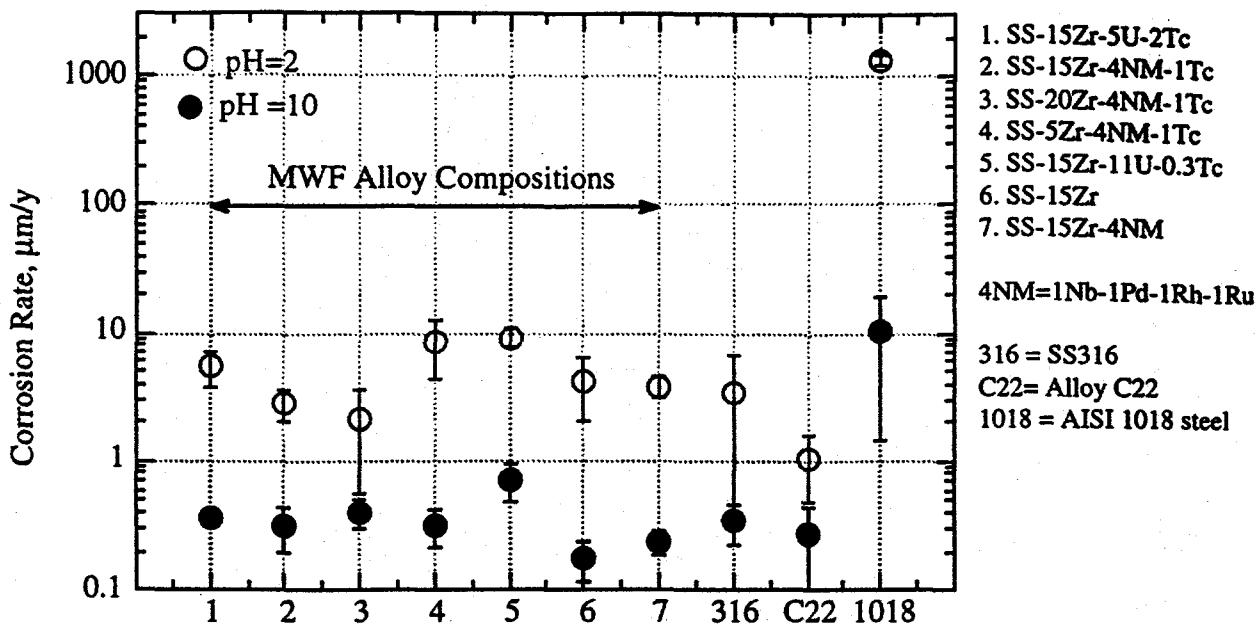

Figure 1. Corrosion rates of various alloys measured by polarization resistance in pH=2 and pH=10 solutions at room temperature.

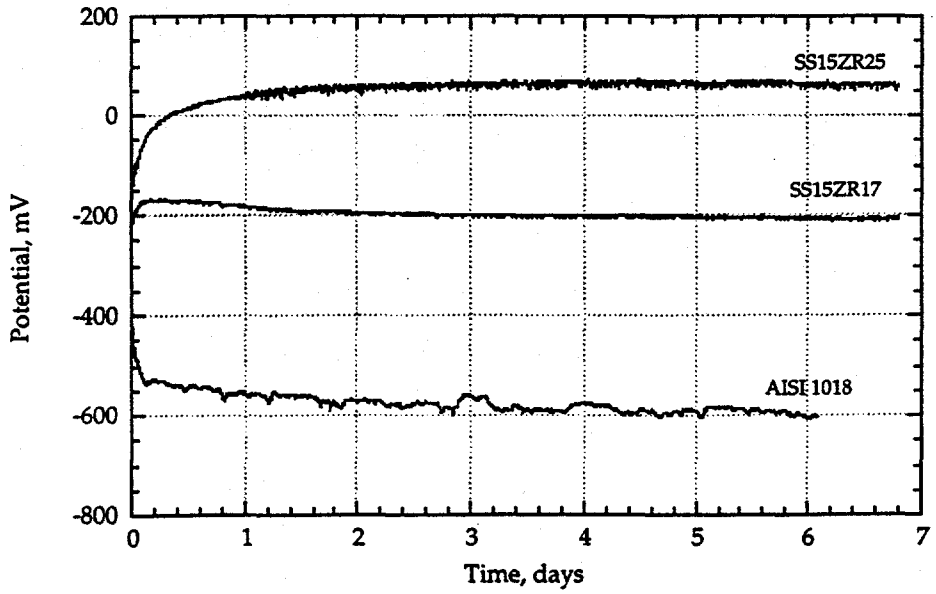

Figure 2. Galvanic Potential (vs. Ag/AgCl reference electrode) at metal specimens coupled to C-22 in J-13 solution.

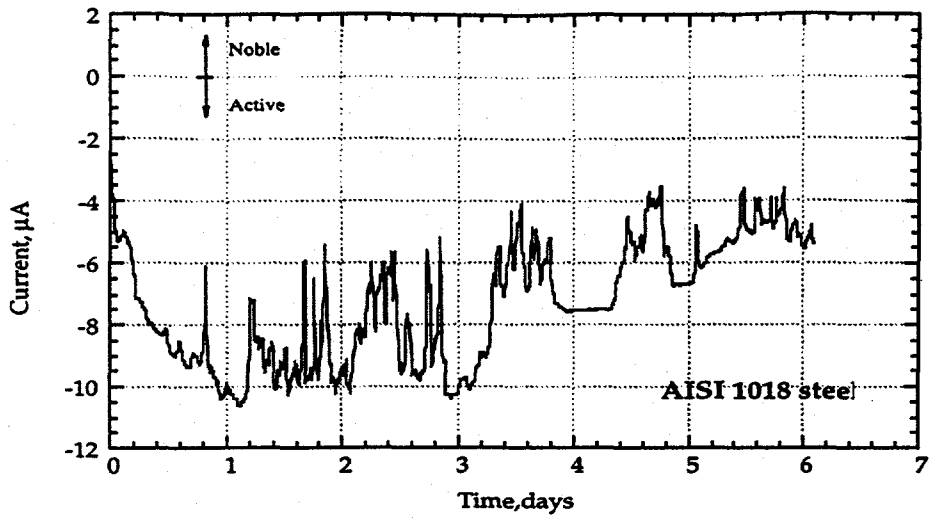

Figure 3. Galvanic current measured for AISI 1018 steel coupled to C-22 in J-13 solution. The steel is electrochemically active compared to C-22.

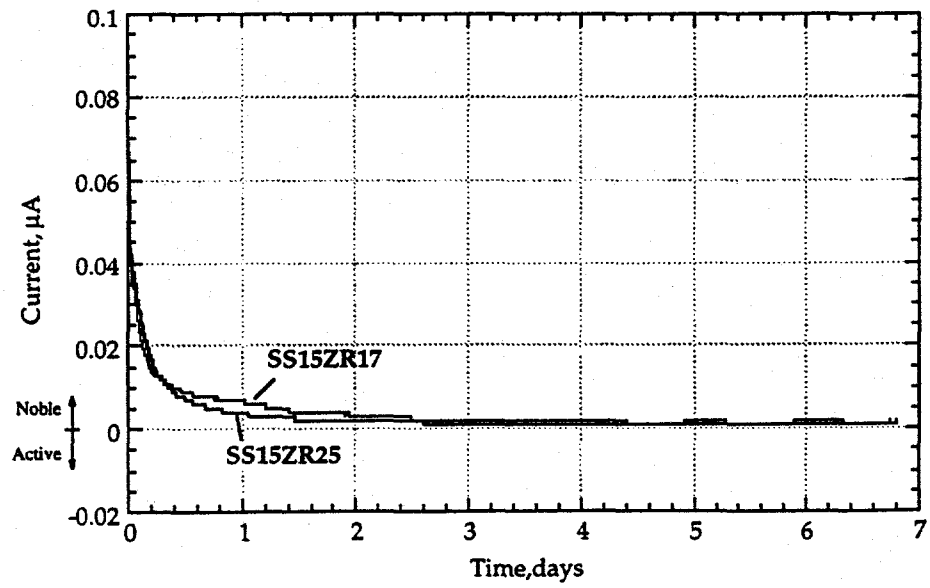

Figure 4. Galvanic current measured for SS15ZR17 and SS15ZR25 specimens coupled to C-22 in J-13 solution. The waste form specimens are noble compared to C-22.

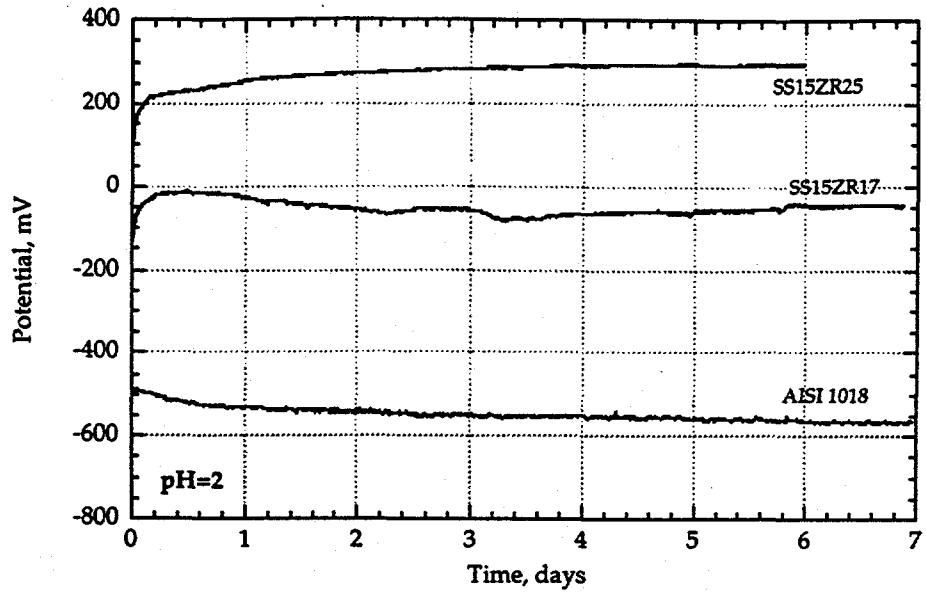

Figure 5. Galvanic potential (vs. Ag/AgCl reference electrode) at metal specimens coupled to C-22 in pH=2 solution.

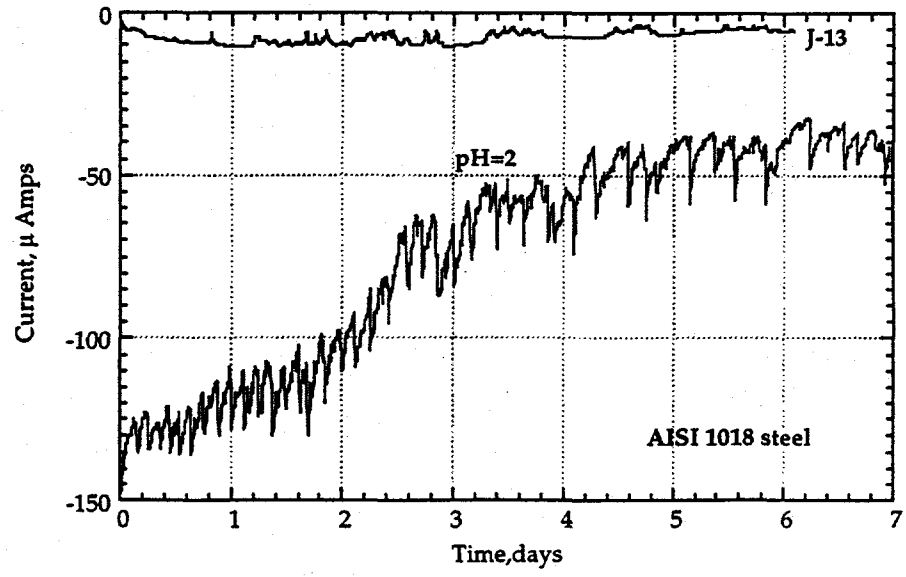

Figure 6. Galvanic currents measured for AISI 1018 steel coupled to C-22 in pH=2 and J-13 solutions.

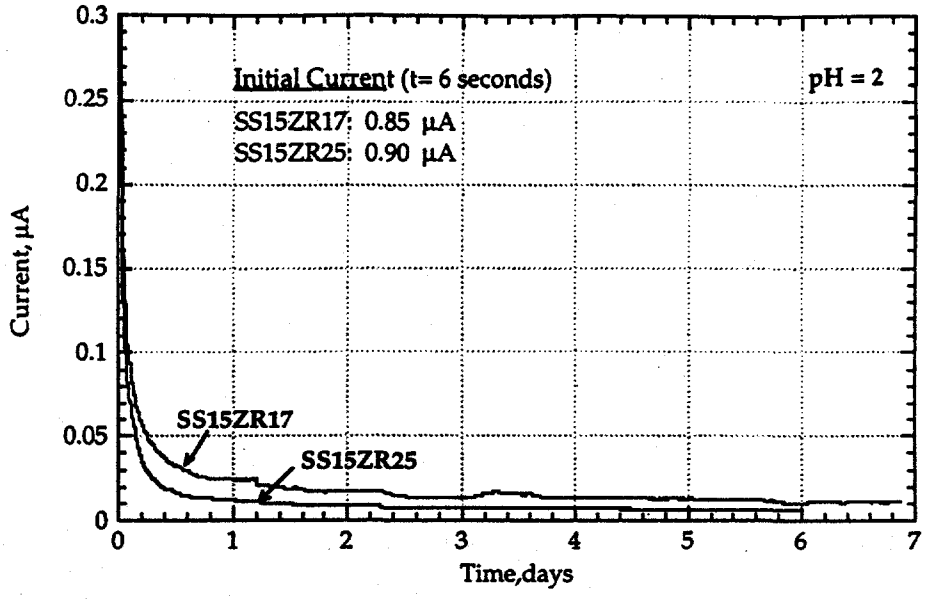

Figure 7. Galvanic current measured for SS15ZR17 and SS15ZR25 specimens coupled to Alloy C22 in pH=2 solution.